A STUDY OF FERRORESONANCE WITH APPLICATION TO DIGITAL LOGIC

by

ALBERT JAMES REED

B.A.Sc., University of British Columbia, 1964

A THESIS SUBMITTED IN PARTIAL FULFILLMENT OF

THE REQUIREMENTS FOR THE DEGREE OF

MASTER OF APPLIED SCIENCE

in the Department of

Electrical Engineering

We accept this thesis as conforming to the

required standard

Research Supervisor

Members of the Committee

Head of the Department

Members of the Department
of Electrical Engineering

THE UNIVERSITY OF BRITISH COLUMBIA

In presenting this thesis in partial fulfilment of the requirements for an advanced degree at the University of British Columbia, I agree that the Library shall make it freely available for reference and Study. I further agree that permission for extensive copying of this thesis for scholarly purposes may be granted by the Head of my Department or by his representatives. It is understood that copying or publication of this thesis for financial gain shall not be allowed without my written permission.

Department of ELECTRICAL ENGINEERING

The University of British Columbia
Vancouver 8, Canada

Date 12 June 1968

ABSTRACT

A series resonant L-C circuit in which either the inductor or the capacitor is nonlinear and which is excited by a sinusoidal voltage of a fixed frequency may have two steady-state responses. One of these responses is characterized by a high amplitude oscillation; the other by a low one. If the amplitude or frequency of the driving signal is varied slowly, the response may suddenly change or "jump" to the other state. As a result, this phenomenon has been called jump resonance, or ferroresonance.

Because the high and low resonant states could be considered as a 0 and 1 basis for digital logic operations, it was the purpose of this work to study the phenomenon and to investigate the possibility of using it in the design of digital logic elements.

Equations which exhibit the necessary features were studied on an analogue computer. The results of the study were used as design criteria for the construction of an actual circuit and also as a basis for an approximate analytical study. The analytical study uses the Ritz method to find useful features of the responses. The results of previous users of this method have been extended to include equations with both second derivative coupling and non-symmetrical nonlinearities.

Based on the above studies, a prototype circuit was designed which has some of the basic properties of conventional

flip-flop circuits. One of the main features of this circuit is that it is almost entirely made of reactive components and as a result has very low power consumption. The operation of the circuit is used to verify the validity of the approximations made in both the analogue simulation and the analytical study. The results obtained from the analogue study, the Ritz analysis, and the prototype circuit compare favorably with each other. Some suggestions for future work are given.

TABLE OF CONTENTS

LIST OF ILLUSTRATIONS

LIST OF SYMBOLS

A,B,C	constants
D	damping coefficient
E	a function
a,c,d,e,h	coefficients
F_o, F_s, F_c	functions
G_o, G_s, G_c	functions
G	amplitude coefficient
f,g	functions
k	a subscript
K	a constant
L	inductance
M	coupling coefficient
η	ω/K
p	amplitude coefficient
q	a variable representing charge
$\tilde{q}$	an approximation to q
μ	nonlinearity coefficient
ψ_k	a set of functions
s	p/K^2
t	a variable, time
τ	ωt
x,y,u,v	variables

$\dot{x}$	dx/dt
$\ddot{x}$	d^2x/dt^2
ω	angular frequency
ω_o	a constant
R	resistance
V	voltage

ACKNOWLEDGEMENT

Grateful acknowledgement is given to the National Research Council of Canada for financial support in the form of a Bursary in 1964-65 and a studentship in 1965-66.

The author wishes to thank his supervisor, Dr. A.C. Soudack for his guidance throughout the course of this work.

Thanks are also given to Dr. M.S. Davies for reading the manuscript and for his useful comments and suggestions, and to Dr. G. Christensen for his helpful discussions.

1. INTRODUCTION

The phenomenon of ferroresonance was observed for the first time in 1906 during the tuning of radio transmitters.[1] Since then it has appeared in the literature pertaining to power systems,[2] electronics,[3] and nonlinear mechanics.[4] Ferroresonance can occur in a driven series resonant circuit which consists of an inductor and a capacitor, one of which is nonlinear. If the nonlinear characteristic is symmetrical, such a circuit can be approximated by Duffing's equation:

$$\ddot{x} + \omega_o^2 x + hx^3 = G \cos \omega t \qquad (1\text{-}1)$$

Closer approximations using higher order terms can be found in Hayashi.[5] This equation has the property that under certain conditions it has two stable solutions near resonance, one a large amplitude oscillation and the other a small one. This phenomenon is called ferroresonance.

The bistable multivibrator, or flip-flop, is one of the most useful electronic devices employed in digital computers. An identifying feature of a bistable multivibrator is that it consists of a pair of two-state devices arranged symmetrically so as to allow only two stable states of the complete circuit. For example, in a transistor flip-flop, either transistor may be on or off but they are arranged so that when one is on it keeps the other off.

It was proposed to investigate the possibility of making a flip-flop type computer component using the ferro-resonant regions of nonlinear L-C circuits. The large amplitude oscillation could represent an on state and the small one an off state. Some work in this area has been done by other workers such as Isborn[6], Gremer[7], and Ozawa[8]. However, their work was based on the assumption of a symmetrical characteristic for the nonlinear element. More recent developments in semiconductors, particularly the advent of varactor diodes, have made it necessary to consider the problem allowing non-symmetrical characteristics.

The work presented here includes the choice of a particular type of nonlinear capacitor, an analogue simulation to obtain a final circuit configuration and to give approximate design values to the components, an approximate mathematical analysis of the circuit, and the building of an operative prototype unit. The circuit finally used can be described by the following equations:

$$\ddot{q}_1 + 2DKg(\dot{q}_1) + K^2 f(q_1) + M\ddot{q}_2 - p \sin \tau = 0$$
$$\ddot{q}_2 + 2DKg(\dot{q}_2) + K^2 f(q_2) + M\ddot{q}_1 - p \sin \tau = 0 \qquad (1\text{-}2)$$

These equations are analyzed using the Ritz or Ritz-Galerkin method. Some of Klotter's[9,10] methods have been extended to equations with second derivative coupling. General algebraic

conditions relating the response to the driving amplitude and frequency are derived for this type of equation. These results are applied to the specific case of a circuit with negligible damping and with an asymmetrical restoring function which can be approximated by:

$$f(q) = q + \mu q^2 \qquad (1\text{-}3)$$

Parametric excitation using the variable capacitance properties of materials such as barium titanate has been achieved[11] and it was thought that components of this type could be used as the nonlinear elements in the synthesis of the proposed circuit. However, they were deemed unsuitable for use at the present time due to their cost and scarcity within the needed capacitance tolerance. Instead, low cost, commercially available silicon capacitors were used to demonstrate the principles of operation and were found to be quite satisfactory.

This thesis consists of a discussion of the analogue computer simulation in Chapter 2, the development of the Ritz analysis in Chapter 3, some discussion of the circuit design and results in Chapter 4, and some suggestions for future study in the concluding Chapter 5.

2. ANALOGUE SIMULATION

2-1 Preamble

An electronic analogue computer consists of a collection of units, each of which is designed to produce an output that is a particular linear or nonlinear function of the inputs. These units are readily interconnected to solve mathematical equations or to simulate the behaviour of a physical system. A convenient feature is on-line control, that is the facility with which changes in parameters of the equations can be made manually during the actual operation or solution of an equation.

2-2 Computer Circuits

The circuit shown in Figure 2-1 can be described by the following equations:

$$V \sin\omega t = L \frac{d^2q_1}{dt^2} + R \frac{dq_1}{dt} + \frac{1}{f(v_{c_1})} q_1 - M \frac{d^2q_2}{dt^2}$$

$$V \sin\omega t = L \frac{d^2q_2}{dt^2} + R \frac{dq_2}{dt} + \frac{1}{f(v_{c_2})} q_2 - M \frac{d^2q_1}{dt^2} \qquad (2\text{-}1)$$

The voltage-capacitance characteristic, $f(v_c)$ is that of a Transitron SC-5 silicon capacitor (Figure 2-2) and was obtained from the manufacturer's specifications and direct measurement. The frequency of the driving sinusoid was chosen to coincide with that of the highest quality factor (Figure 2-3) at about 2×10^6 r/s. An estimate was made of the maximum probable

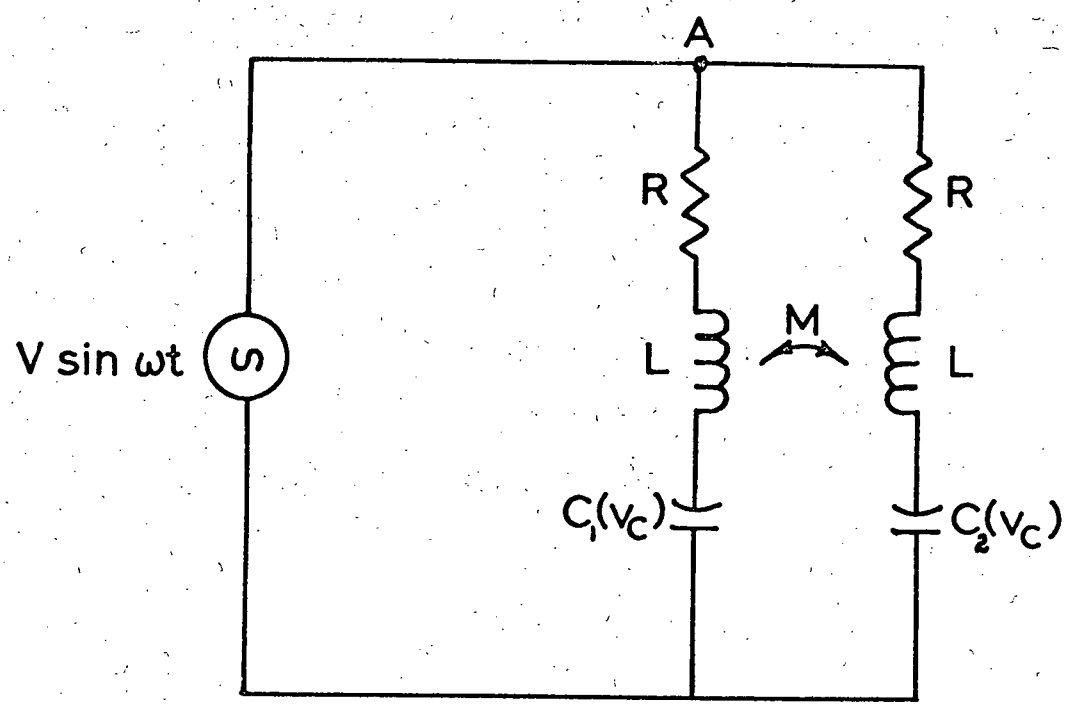

Figure 2.1 Basic Coupled Circuit

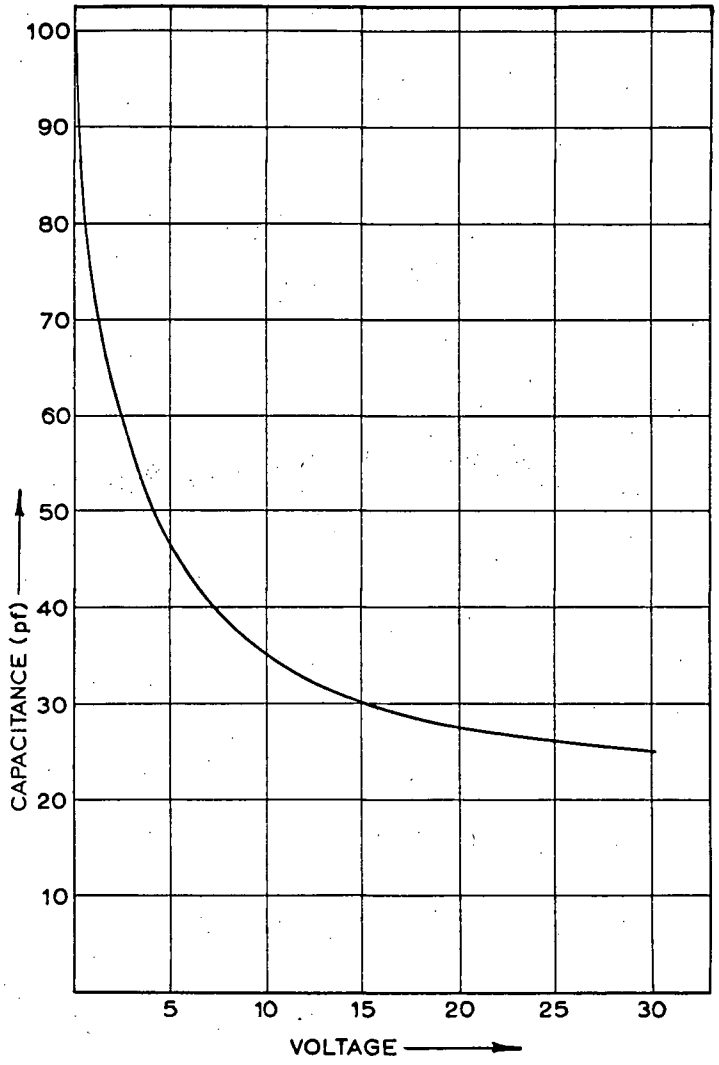

Figure 2.2 Silicon Capacitor Characteristics

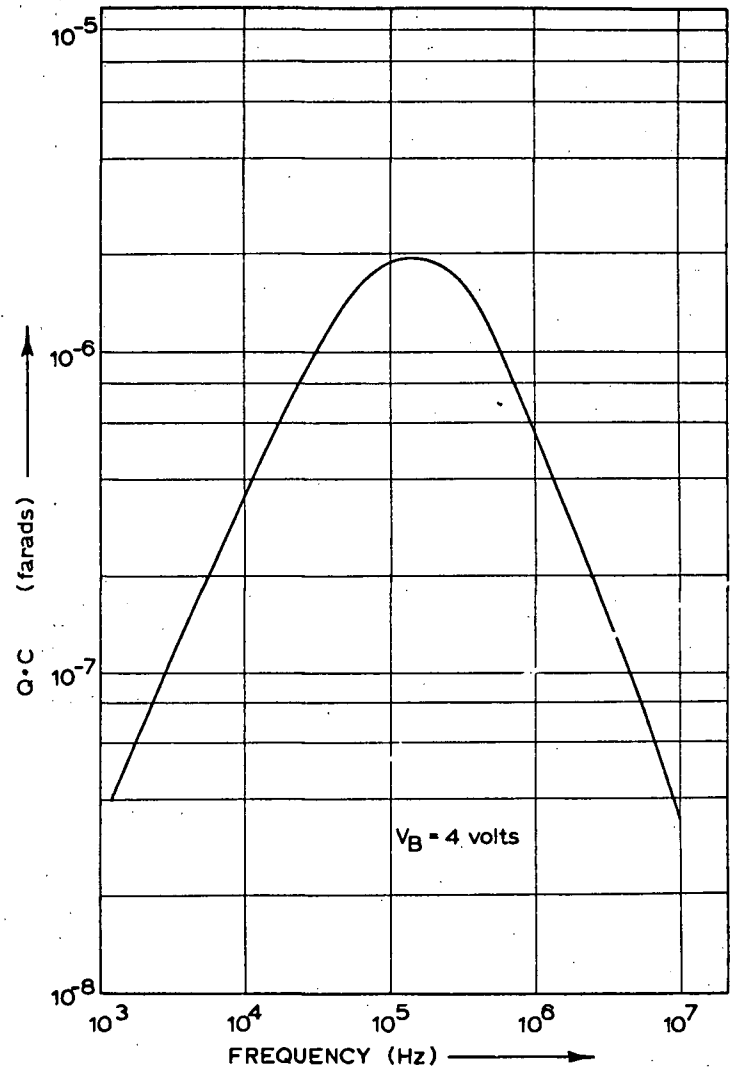

Figure 2.3 Quality Factor for Silicon Capacitors

value of all the variables and of their first and second derivatives. Amplitude and time scaling transformations were then made on (2-1) so that no variable or its derivatives would exceed unity and also so that the operating frequency would be about two cycles/sec. These operations are necessary to prepare an equation for solution on an analogue computer.

The sinusoidal forcing function was obtained by solving a Van der Pol type of equation:[12]

$$\ddot{x} - 10(A^2 - x^2 - (\frac{\dot{x}}{\omega})^2)\,\dot{x} + \omega^2 x = 0 \qquad (2\text{-}2)$$

$$x(0) = A, \qquad \dot{x}(0) = 0$$

This equation has the solution

$$x = A \cos \omega t \qquad (2\text{-}3)$$

and has the property that if perturbed, the solution will quickly return to (2-3), and it will not decay due to leakage in the computer capacitors or other non-ideal factors.

This can readily be seen by an examination of the sign of the damping coefficient in (2-2). The circuit used to solve 2-2 is shown in Figure 2-4. The circuit used to solve the time and amplitude scaled (2-1) is shown in Figure 2-5. There were various minor modifications and additions to this circuit to allow sign changes of M/L, inclusion of source impedance, various input disturbances, and some protective precautions, but these are all omitted in Figure 2-5 for the sake of clarity.

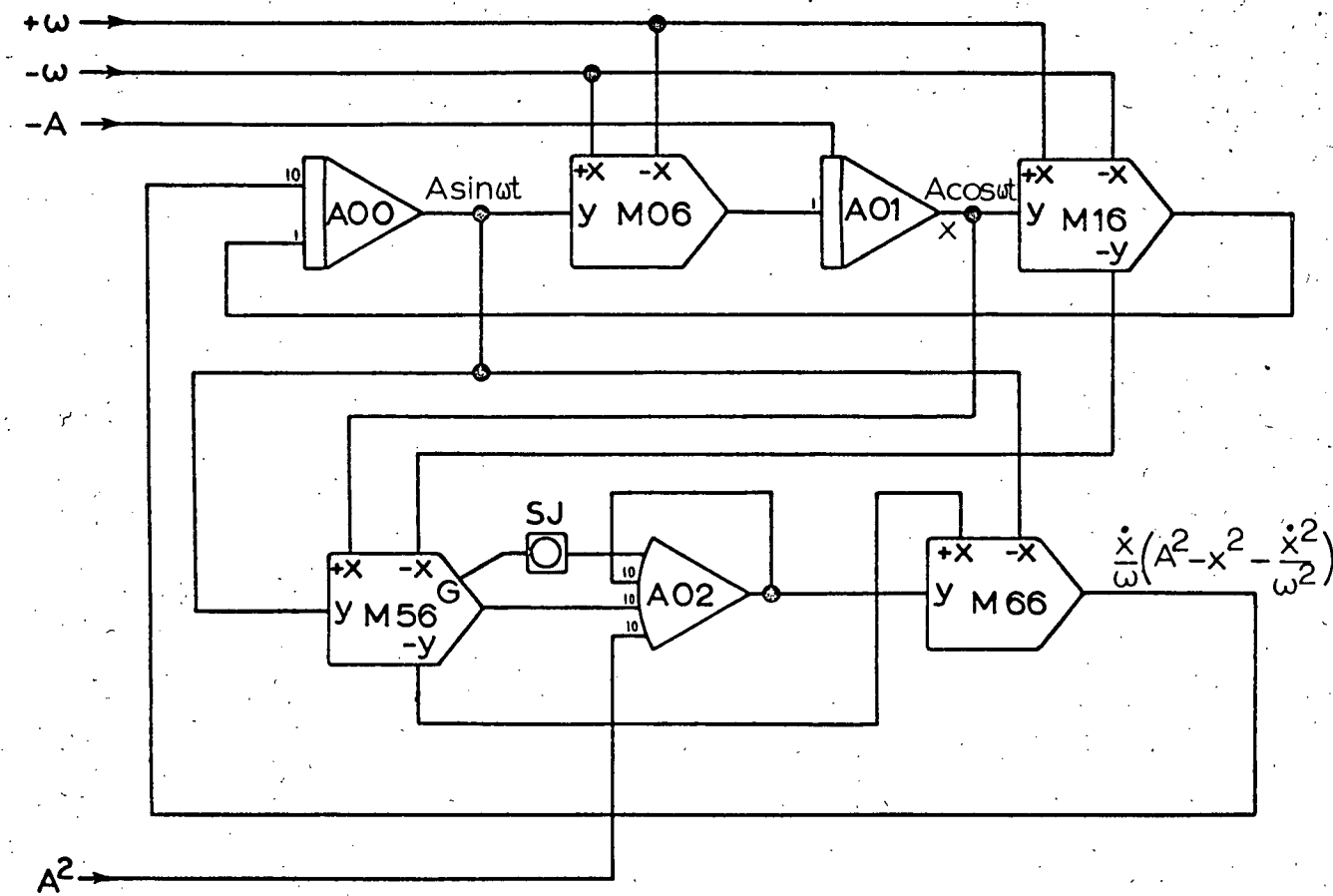

Figure 2.4 Forcing Function Generator

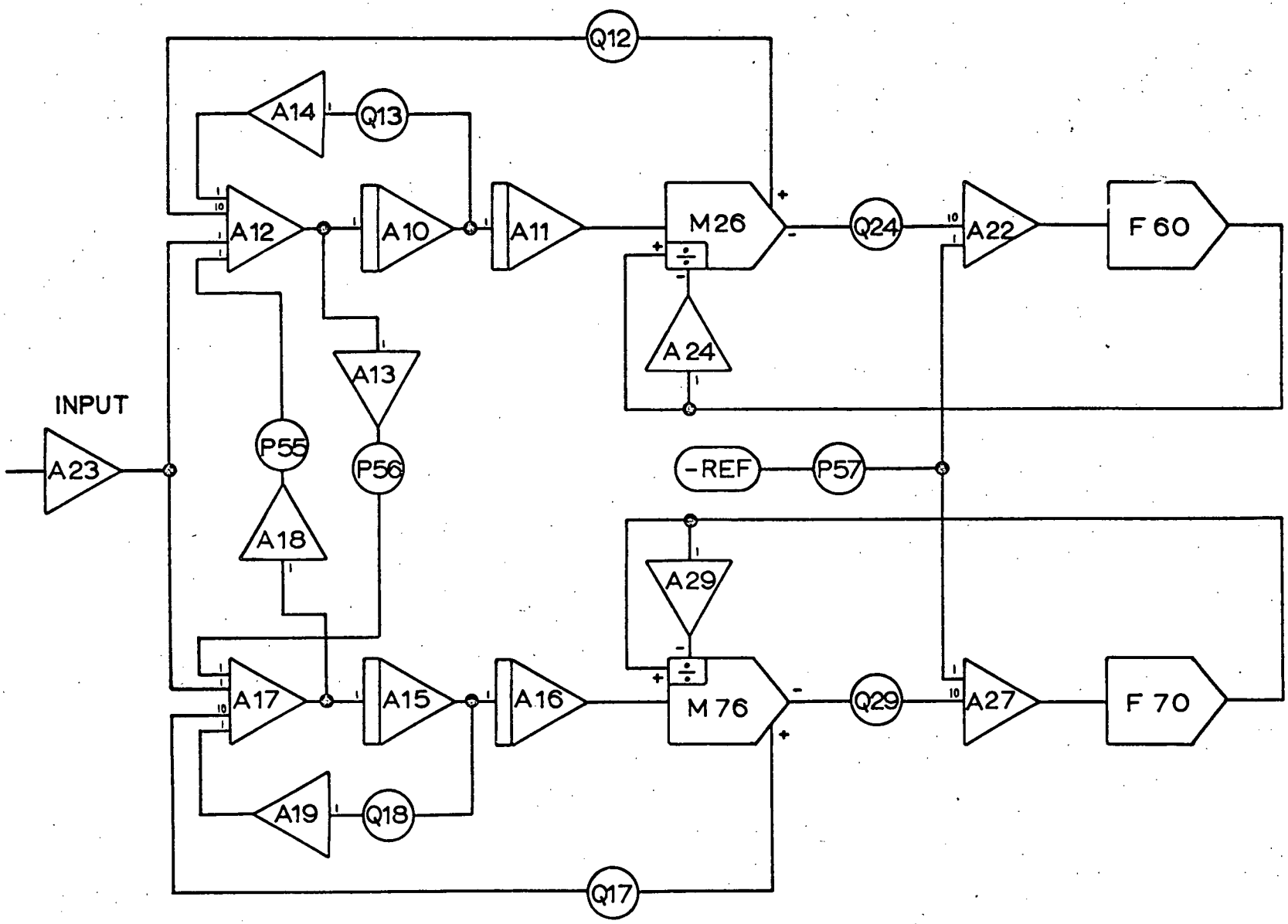

Figure 2.5 Similation of Basic Coupled Circuit

2-3 Discussion of Analogue Computer Results

(a) Form of Solutions

The results obtained on the Pace 231-R computer proved very useful in determining component values for the final circuit. Examples of solutions are given in Figures 2-6 through 2-11. From the results, several features are apparent. Firstly, it can be seen that the solution is approximately a biassed sinusoid with the same frequency as the driving function in most cases. Subharmonics will be discussed separately. Secondly, it is clear that jump resonance can occur. This means that for the same driving function, there can be two possible states of each side of the circuit of Figure 2-1. This feature is shown in Figure 2-6 where the upper trace is the input driving function which is kept constant, and the lower trace is proportional to the voltage across one of the silicon capacitors. The jump or transition between the two states was initiated by a small pulse applied to amplifier A22 which simulated a pulse in the bias of one of the capacitors of Figure 2-1, thus causing a momentary change in the average capacitance.

Figures 2-7, 2-8 and 2-9 show the possibility of the existence of subharmonics[5]. It was somewhat difficult to initiate this mode of resonance, but by various on-line disturbances of the solution, subharmonics of this type could be made to exist. Once initiated, they were maintained indefinitely.

However, because of the peaked shape of Figure 2-3, it is most unlikely that any subharmonics could persist in the actual circuit of Figure 2-1 because of the greater damping at higher and lower frequencies, a feature not included in the analogue model.

(b) Effect of Varying the Resistance

The coefficient representing the resistance of Figure 2-1 was readily varied by changing potentiometers Q13 and Q18 of Figure 2-5. It was found that for the first derivative coefficient value of above about 0.2 there was no jump resonance. This value represented a series resistance of about 17 ohms in the circuit being modelled. Progressively smaller values of this coefficient gave an increase in the ratio between high and low states and also a decrease in the switching time between the two states. However, there was also an increase in the time required for the transient modulation to damp out. This feature is shown in Figure 2-10 which is the transition between high and low states with a damping coefficient of 0.04. Note that the modulation of the carrier envelope after the jump is very similar to the overshoot in an underdamped linear second order system. Note also that the jump occurs in six cycles of the carrier instead of the eleven cycles in Figure 2-6 where the damping coefficient is 0.05 and the thirteen cycles in Figure 2-11 where the damping coefficient is 0.07. Thus it is seen that to build the desired circuit,

the loss must be kept low enough to allow ferroresonance, but not so low as to permit excessive transient modulation of the output waveform during switching intervals.

(c) Effect of Varying the Coupling

One of the main reasons for studying a model of the circuit (Figure 2-1) on the analogue computer rather than using the actual circuit was the ease with which the M/L ratio could be varied. Potentiometers P55 and P56 controlled the coupling between the branches. Amplitude and frequency responses were obtained for various values of the M/L ratio. It was found that up to a point, increasing this ratio increased the region in which the entire coupled circuit could be symmetrically bistable; that is, when one branch of the circuit is in the high state, the other will be in the low one (see Figure 2-11). However, if this ratio was increased beyond about 0.3, the two branches became tightly coupled so that they would both be in either the high state or the low state - - a symmetrically bistable state was not possible. Hence it is seen that if the M/L ratio is too small, the circuit must be very accurately tuned to be bistable at all, but if the ratio is too large the desired symmetrically bistable state cannot exist. An M/L value of 0.1 was found to be a good compromise.

2-4 Summary of the Analogue Simulation Results

The simulation of various circuits on the analogue computer provided invaluable groundwork for the chapters to

follow. Firstly, the basic circuit configuration to be used was determined. Secondly, the general shape and features of the output waveform were found. Knowledge of these is necessary for the Ritz analysis in the next chapter. Also, study of the analogue circuit gave the design criteria for M, L, and R that are used later in this work. The most important result of this simulation, albeit intangible, was the intuitive understanding which it gave of the circuit.

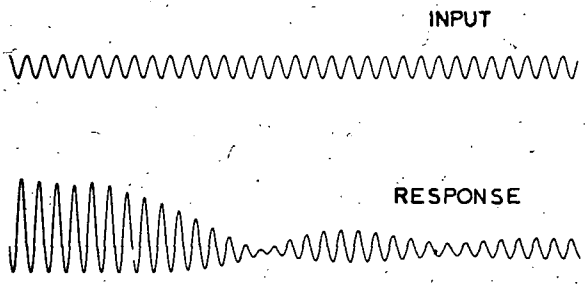

Figure 2.6

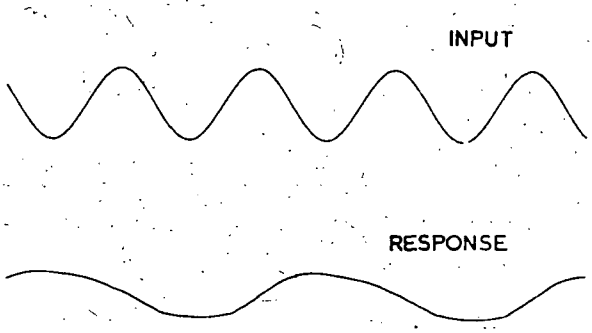

Figure 2.9

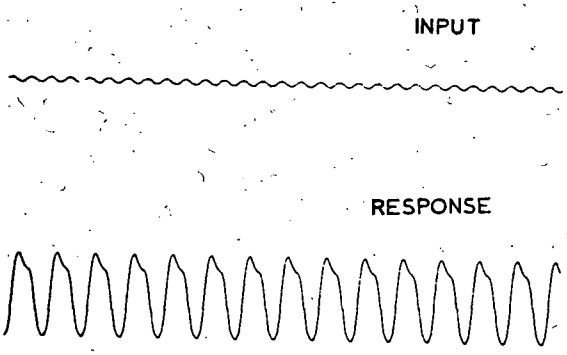

Figure 2.7

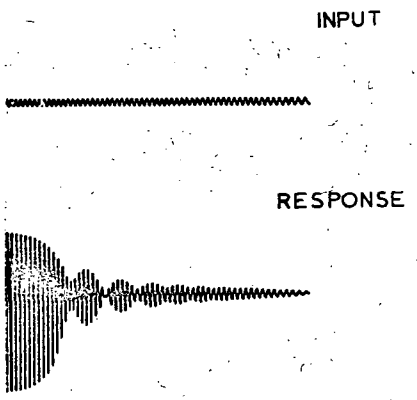

Figure 2.10

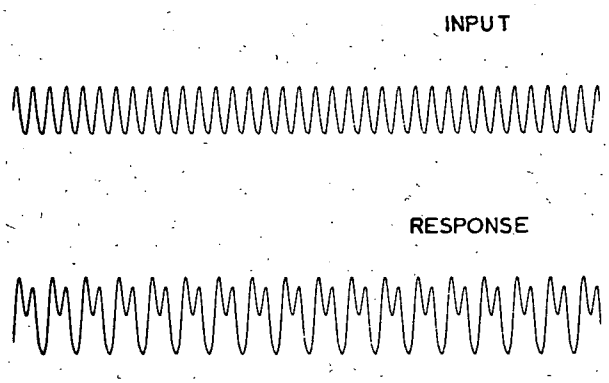

Figure 2.8

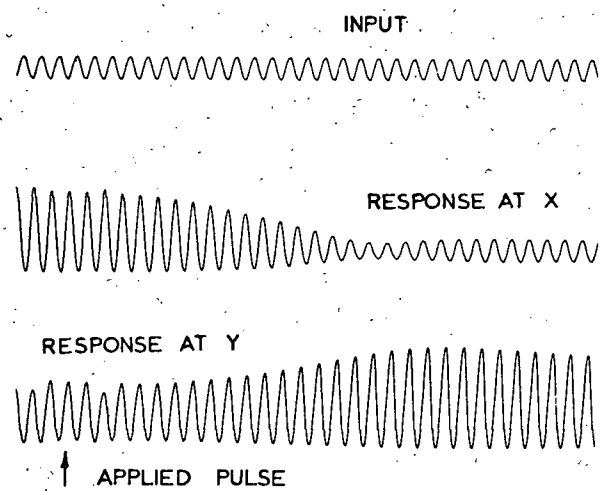

Figure 2.11

3. CIRCUIT ANALYSIS AND DESIGN

3-1 Preamble

When considering the behaviour of linear systems, it is convenient to deal with sinusoidal inputs and their outputs which are again sinusoidal. As a result of the principle of superposition, the ratio between output and input as a function of frequency is a basis for a complete description of the system behaviour. However, in nonlinear systems this principle cannot be used[13] and other methods, which are usually approximations, must be found. In the following analysis, the Ritz[14] or Ritz-Galerkin method will be used. This method is capable of handling a large variety of steady state cases. The main difficulty involved in using the Ritz method is that the approximate form of the solution must be known or assumed. As a result, this method will not find unknown features of the solution such as higher or lower harmonics if they are not included in the assumed solution. The results of the analogue computer study show that a biassed sinusoid at the forcing frequency is a good approximation to the solution waveform, and such a solution can be well approximated with the Ritz method.

3-2 The Ritz Method as Applied to Forced Oscillations

The Ritz method, as summarized by Klotter[9], is based on the following principle. Let the differential equation

describing a system be:

$$E\left[q(t)\right] = 0 \tag{3-1}$$

and replace the solution, $q(t)$, by an assumed form:

$$\tilde{q}(t) = \sum_{k=1}^{m} a_k \psi_k(t) \quad \text{for } a < t < b \tag{3-2}$$

where the $\psi_k(t)$ are an appropriately chosen set of linearly independent functions. Unless $\tilde{q}(t)$ is the exact solution, $E\left[\tilde{q}(t)\right]$ will not vanish. The Ritz conditions for the system are conditions on a_k such that

$$\int_a^b E\left[\tilde{q}(t)\right] \psi_k(t)dt = 0 \quad (k=1,2,\ldots m) \tag{3-3}$$

3-3 Development of the Ritz Conditions

The equations to be considered describe the circuit of Figure 2-1 and are of the form:

$$E\left[q_1\right] \triangleq \ddot{q}_1 + 2DKg(\dot{q}_1) + K^2 f(q_1) + M\ddot{q}_2 - p \sin \tau = 0 \tag{3-4a}$$

$$E\left[q_2\right] \triangleq \ddot{q}_2 + 2DKg(\dot{q}_2) + K^2 f(q_2) + M\ddot{q}_1 - p \sin \tau = 0 \tag{3-4b}$$

where $\tau = \omega t$.

We can choose our ψ_k to give assumed approximate solutions of the form:

$$\tilde{q}_1 = C_1 + A_1 \sin \tau - B_1 \cos \tau \tag{3-5a}$$

$$\tilde{q}_2 = C_2 + A_2 \sin\zeta - B_2 \cos\zeta \qquad (3\text{-}5b)$$

where C_1 and C_2 are included to allow for possible asymmetry in the f or g functions. It follows that

$$\dot{\tilde{q}}_i = \omega A_i \cos\zeta + \omega B_i \sin\zeta \qquad i = 1,2 \quad (3\text{-}6a)$$

$$\ddot{\tilde{q}}_i = -\omega^2 A_i \sin\zeta + \omega^2 B_i \cos\zeta \qquad i = 1,2 \quad (3\text{-}6b)$$

By defining auxiliary functions

$$F_o^i(C_i, A_i, B_i) \triangleq \int_0^{2\pi} f(\tilde{q}_i)\,d\zeta \qquad i = 1,2 \quad (3\text{-}7a)$$

$$F_s^i(C_i, A_i, B_i) \triangleq \int_0^{2\pi} f(\tilde{q}_i)\sin\zeta\, d\zeta \qquad i = 1,2 \quad (3\text{-}7b)$$

$$F_c^i(C_i, A_i, B_i) \triangleq \int_0^{2\pi} f(\tilde{q}_i)\cos\zeta\, d\zeta \qquad i = 1,2 \quad (3\text{-}7c)$$

$$G_o^i(A_i, B_i, \omega) = \frac{1}{K}\int_0^{2\pi} g(\dot{\tilde{q}}_i)\,d\zeta \qquad i = 1,2 \quad (3\text{-}8a)$$

$$G_s^i(A_i, B_i, \omega) = \frac{1}{K}\cdot\frac{1}{\pi}\int_0^{2\pi} g(\dot{\tilde{q}}_i)\sin\zeta\, d\zeta \qquad i = 1,2 \quad (3\text{-}8b)$$

$$G_c^i(A_i, B_i, \omega) = \frac{1}{K}\cdot\frac{1}{\pi}\int_0^{2\pi} g(\dot{\tilde{q}}_i)\cos\zeta\, d\zeta \qquad i = 1,2 \quad (3\text{-}8c)$$

the Ritz conditions:

$$\int_0^{2\pi} E\left[\tilde{q}_i\right] d\zeta = 0 \qquad i = 1,2 \qquad (3\text{-}9a)$$

$$\int_0^{2\pi} E\left[\tilde{q}_i\right] \sin\zeta \, d\zeta = 0 \qquad i = 1,2 \tag{3-9b}$$

$$\int_0^{2\pi} E\left[\tilde{q}_i\right] \cos\zeta \, d\zeta = 0 \qquad i = 1,2 \tag{3-9c}$$

give rise to the following set of algebraic equations:

$$\left.\begin{aligned} F_o^i + 2DG_o^i &= 0 && \text{(3-10a)}\\ F_s^i + 2DG_s^i - \eta^2 A_i - M\eta^2 A_j - S &= 0 && \text{(3-10b)}\\ F_c^i + 2DG_c^i + \eta^2 B_i + M\eta^2 B_j &= 0 && \text{(3-10c)} \end{aligned}\right\} \begin{array}{l} i=1,2 \\ j=1,2 \\ i \neq j \end{array}$$

where $S = p/K^2$ and $\eta = \omega/K$.

The f(q) characteristic for the silicon capacitors used may be approximated (see Appendix A) by:

$$f(q) = q + \mu q^2 \tag{3-11}$$

Using (3-11), we obtain the following Ritz conditions for the coupled, non-symmetric equations:

$$\left.\begin{aligned} F_o^i + 2DG_o^i &= 0 && \text{(3-12a)}\\ F_s^i + 2DG_s^i - \eta^2 A_i - M\eta^2 A_j - s &= 0 && \text{(3-12b)}\\ F_c^i + 2DG_c^i + \eta^2 B_i + M\eta^2 B_j &= 0 && \text{(3-12c)} \end{aligned}\right\} \begin{array}{l} i=1,2 \\ j=1,2 \\ i \neq j \end{array}$$

If we evaluate F_c^i from equation (3-7c) we obtain:

$$F_c^i = B_i(2\mu C_i - 1) \tag{3-13}$$

It is evident now, that if we assume negligible damping (i.e. $D \simeq 0$), equation (3-12c) is satisfied for $B_i = B_j \equiv 0$. For this case, our simplified Ritz conditions become:

$$2C_i + 2\mu C_i^2 + \mu A_i^2 = 0 \qquad \left.\begin{matrix} i = 1,2 \\ j = 1,2 \\ i \neq j \end{matrix}\right\} \qquad (3\text{-}14a)$$

$$A_i(1 + 2_\mu C_i) - \eta^2 A_i - M\eta^2 A_j - S = 0 \qquad (3\text{-}14b)$$

Solving for C_i in (3-12b) and substituting in (3-12a) yields equations of the form:

$$x^4 + bx^2 + cx + dxy + ey^2 + hy + a = 0 \qquad (3\text{-}15)$$

$$y^4 + by^2 + cy + dxy + ex^2 + hx + a = 0 \qquad (3\text{-}16)$$

where

$$x = A_1 \qquad d = \frac{M\eta^4}{\mu^2}$$

$$y = A_2 \qquad e = \frac{M\eta^4}{2\mu^2}$$

$$b = \frac{\eta^4 - 1}{2\mu^2} \qquad h = \frac{M\eta^2 s}{\mu^2}$$

$$c = \frac{s\eta^2}{\mu^2} \qquad a = \frac{s^2}{2\mu^2}$$

Making the substitutions $x = u + v$, $y = u - v$ and adding and subtracting (3-15) and (3-16) uncouples the equations and gives:

$$v \cdot \left[4ur^2 + 2(b-e)\, u + c-h \right] = 0 \qquad (3\text{-}17)$$

$$r^4 + 4u^2(r^2-u^2) + br^2 + cu + d(2u^2-r^2) + er^2 + hu + a = 0 \qquad (3\text{-}18)$$

where $r^2 = u^2 + v^2$. Equation (3-17) is satisfied if $v = 0$. If $v \neq 0$, solving for r^2 in (3-17) and using this value

in (3-16) gives a polynomial in powers of u:

$$u^6\left[-4\right] + u^4\left[2(d + e - b)\right] + u^3\left[2h\right] + u^2\left[3e^2 - b^2 + 2bd - 2dc - 2be + 4a\right].\tfrac{1}{4} + u\left[\left(\frac{e}{2} - \frac{d}{4}\right).(h - c)\right] + \frac{1}{16}\left[h - c\right]^2 = 0 \qquad (3\text{-}19)$$

When $v = o$, $x = y$ and equation (3-15) may be solved directly. When $v \neq o$ the Ritz coefficients are determined from the roots of (3-19).

3-4 Qualitative Discussion of Solutions

To get an heuristic idea of what to expect for solutions, it is useful to examine (3-14a) and (3-14b) more closely. Solving for C_i in the first equation gives

$$C_i = \frac{-1 \pm \sqrt{1 - 2\mu^2 A_i}}{2\mu} \quad (i = 1,2) \qquad (3\text{-}20)$$

Now if A_i is zero, C_i must also be zero because there is no oscillation to cause the bias or dc term. Thus, only the positive sign in front of the radical in (3-20) is meaningful. The negative sign leads to extraneous roots. Using (3-20), substituting for C_i in (3-14b), and solving for η^2 yields:

$$\eta^2 = \frac{1}{\left(1 + M\frac{A_i}{A_i}\right)}\left[\sqrt{1 - 2\mu^2 A_i^2} - \frac{S}{A_i}\right] \qquad (3\text{-}21)$$

In the special case where $M = 0$, these equations reduce to exactly the same form as given by Klotter[9] for uncoupled equations. Figure 3-1(a) is a typical frequency response plot of (3-21) for $M = 0$. For $M \neq 0$, the term $1/(1 + M\frac{A_i}{A_i})$ expands or

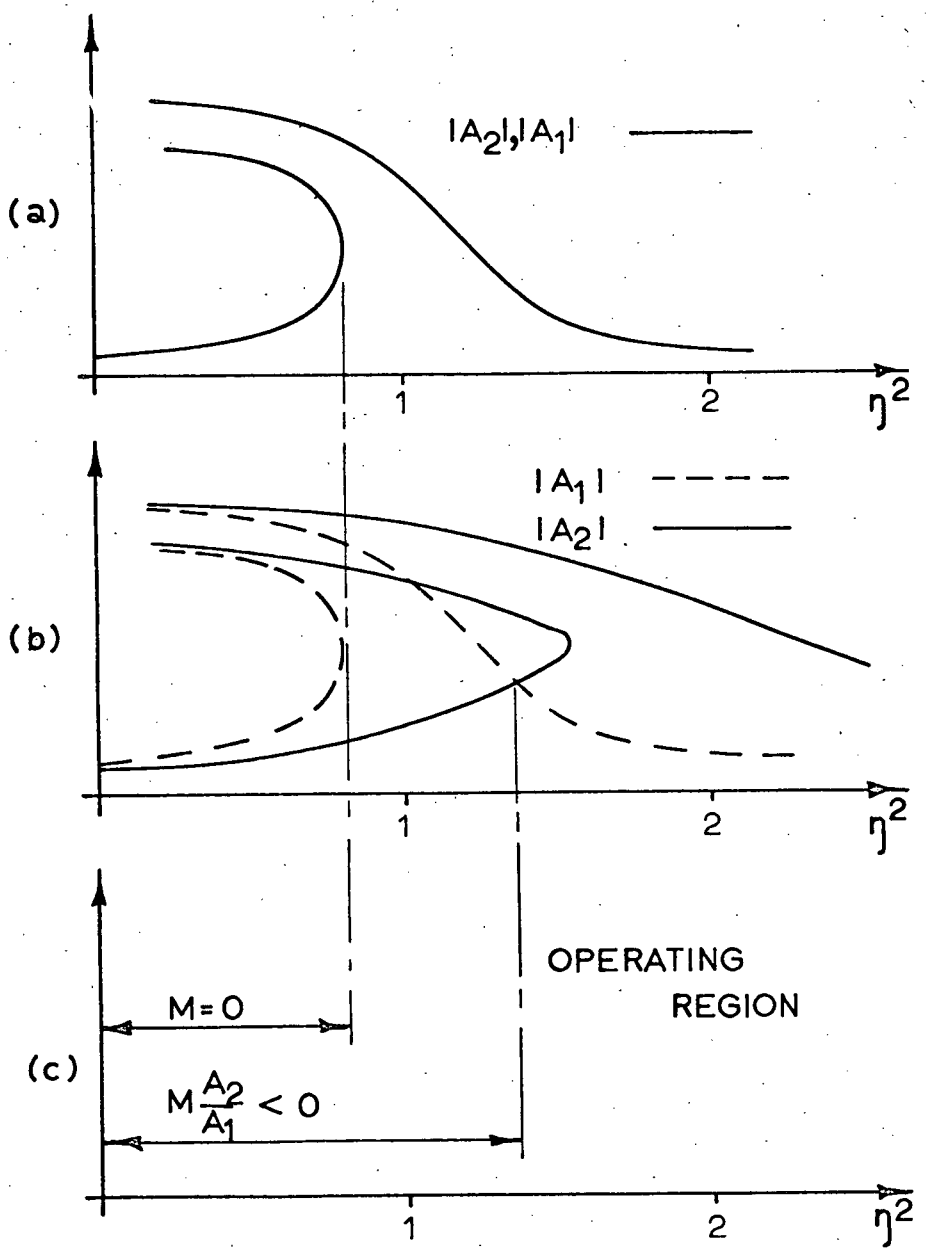

Figure 3.1 Typical Frequency Responses

contracts this curve along the η^2 axis. The curves shown in Figure 3-1(b) depict this feature and are drawn assuming that A_i is greater than A_j and that $M \frac{A_j}{A_i}$ is slightly greater than -1. Because $(1 + M \frac{A_i}{A_j})$ is smaller than $(1 + M \frac{A_j}{A_i})$, the curve for $i = 2$, $j = 1$ is expanded along the η^2 axis more than the curve for $i = 1$, $j = 2$. Thus the possible operating region where A_1 is greater than A_2 is increased as shown in Figure 3-1(c). With $M \frac{A_1}{A_2}$ positive, the possible operating region is decreased.

3-5 Features of the Solutions

A more thorough and quantitative determination of the Ritz coefficients is obtained by solving (3-16) and (3-19) directly. There are sixteen root pairs resulting from these equations. Four are obtained from the solution of (3-16) for the case $x = y$. The other twelve are solutions of the sixth order (3-19) and the transformation $r^2 = u^2 + v^2$ in (3-18). However, because of the symmetry involved, for each of six x, y solution pairs resulting from (3-19) there is an identical y, x solution. The equations were solved on an I.B.M. 7040 digital computer using Laguerre's method[15],[16] for extracting polynomial roots, (see Appendix B). This method was found to be more reliable for this work than the Muller, Newton, or Bairstow methods. The Ritz coefficients were determined and their dependence on the driving amplitude s, the normalized frequency η, and the coupling term M were found. Examples of the solutions which come from the real roots of (3-16) and (3-19) are given

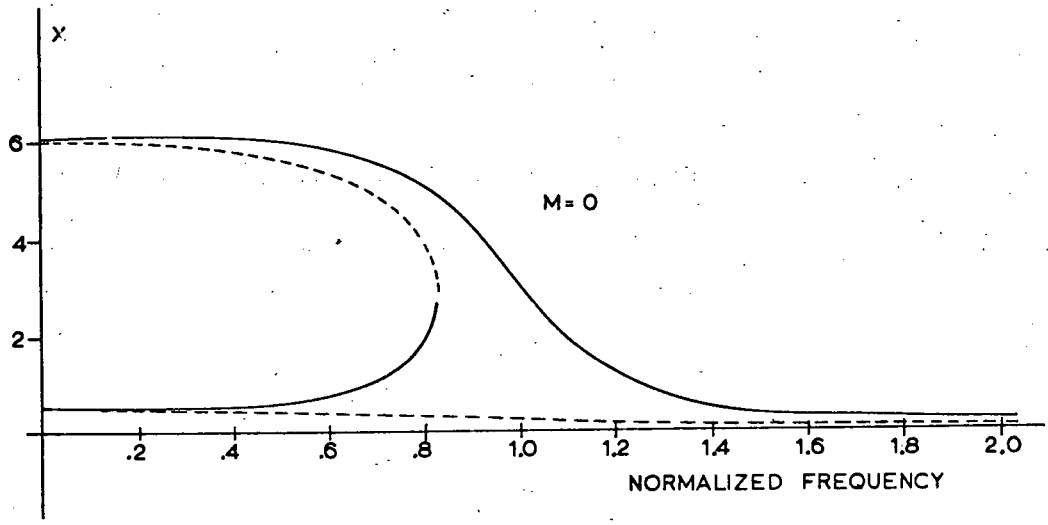

Figure 3.2 Frequency Response for Uncoupled Case

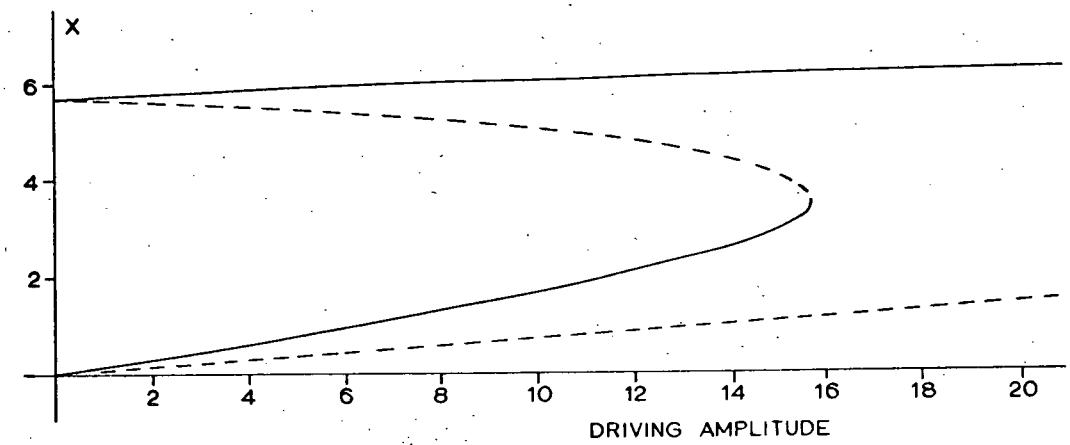

Figure 3.3 Amplitude Response for Uncoupled Case

in Figures 3-2 through 3-8. Complex roots have no physical meaning.

3-6 Discussion of the Uncoupled Case (M = 0)

(a) Frequency Characteristics

In Figure 3-3 it is seen that the frequency response of this nonlinear circuit is quite unlike that of its linear counterpart-two series resonant L-C circuits. The curve is shaped so that although the system described is lossless, the response is everywhere finite. Also, as previously mentioned, the circuit can exist in more than one state at a given driving frequency. It can be shown[5],[8] that solutions characterized by negative slope regions in the $|x|$ - s plane are unstable and hence cannot exist in a physical system. These solutions and the ones resulting from extraneous roots are shown in broken lines in the figures. It is seen then, that for the uncoupled case, the circuit can exist in four different states: a 1-1 state (both x and y large and opposite in phase to the driving term); a 0-0 state (both x and y small and in phase with the driving term); a 1-0 state; and a 0-1 state.

(b) Amplitude Characteristics

Figure 3-3 shows that the dependence of the responses on the driving amplitude is also quite unlike that of the circuit's linear counterpart. The dependence is examined at a frequency that is known from Figure 3-2 to have more than one possible response. Again, the unstable and extraneous solutions are shown with broken lines. It is seen that if the circuit is

in the 0-0 state and the driving amplitude is gradually increased, the response increases gradually until the vertical tangent point on the lower curve is reached, and then suddenly increases to the amplitude and phase given by the upper curve (a 1-1 state). From then on, the response gradually increases with increasing input amplitude.

(c) Effect of Damping

The effect of slight loss in the resonant circuit can be shown[5] to modify the previously discussed curves as depicted in Figures 3-4 and 3-5. It is seen that if the circuit is again in the 0-0 state and the input amplitude is gradually increased, the response increases and a jump in amplitude and phase occurs as before. If now the amplitude is slowly decreased, the response decreases slowly until the other vertical tangency point is reached at which time the circuit reverts to the 0-0 state. In the region between the two vertical tangent points, all four states are possible. The change of state with driving amplitude is discussed in 3-8 as a means of limiting the number of stable states.

If the circuit is more heavily damped so that no vertical tangent points occur, the two sides of the circuit cannot be in different states.

3-7 The Effect of Coupling

It is useful first to consider a typical response plot as shown in Figure 3-6. This plot is the entire solution from

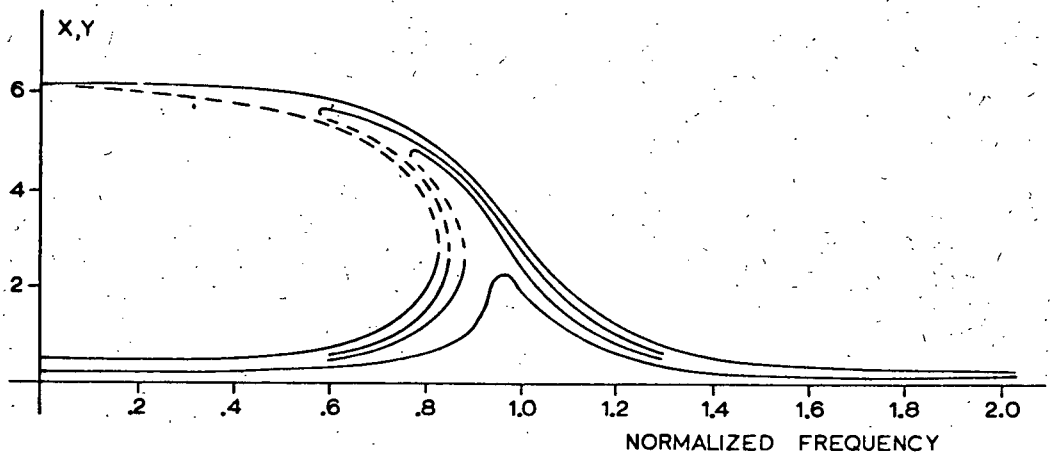

Figure 3.4 Effect of Damping on Frequency Response

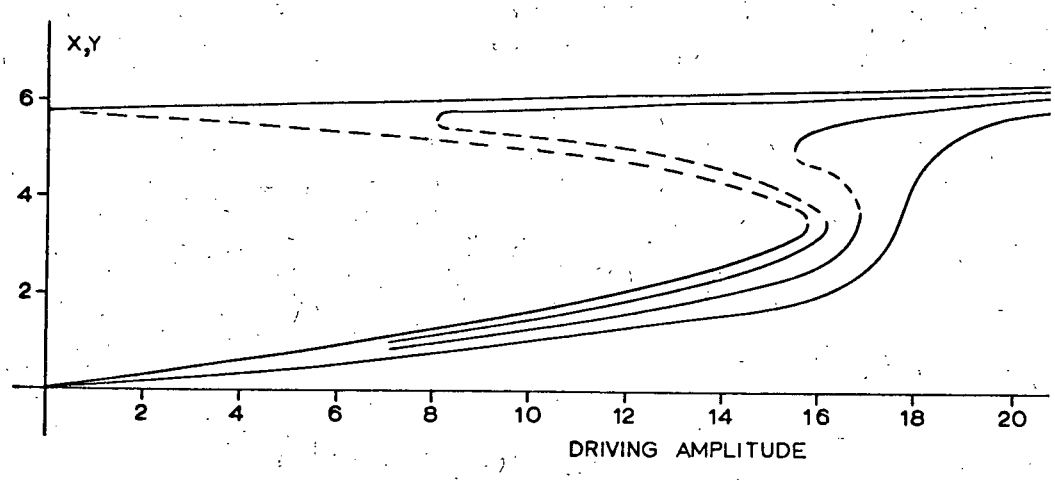

Figure 3.5 Effect of Damping on Amplitude Response

equation (3-19) as it varies with driving amplitude. The six x, y pairs shown are labelled (x_1,y_1) through (x_6,y_6). It should be remembered that there are six more pairs (x_7,y_7) through (x_{12},y_{12}) but these are the same as (x_1,y_1) through (x_6,y_6). The unstable and extraneous solutions are again shown in broken lines and it should be noted that only x_1,y_1 is left solid and hence is the only solution of interest. In the following discussion only the solutions of interest will be shown.

The effect of varying M is then seen by examining the frequency plots of Figures 3-7 and 3-8. It is seen that greater coupling with M positive results in a decreased region of possible bistability with both sides of the circuit in the same state (0-0 or 1-1). Also, it results in a greater region of possible symmetrical bistability (0-1 or 1-0). With M negative, the opposite effect is observed, that is the unsymmetrical region (0-0 or 1-1) is increased whereas the symmetrical region is decreased. It should be possible then, to have the circuit operate at a point such that only the desired symmetrical states can exist.

3-8 Source Impedance Considerations

Consider the effect of placing a capacitor, C_s in series with the carrier source of the circuit shown in Figure 2-1 which was previously discussed. Let the source voltage, V, be increased such that when the circuit is in either the 0-1 or 1-0 state, the voltage at A is the same as it was before the

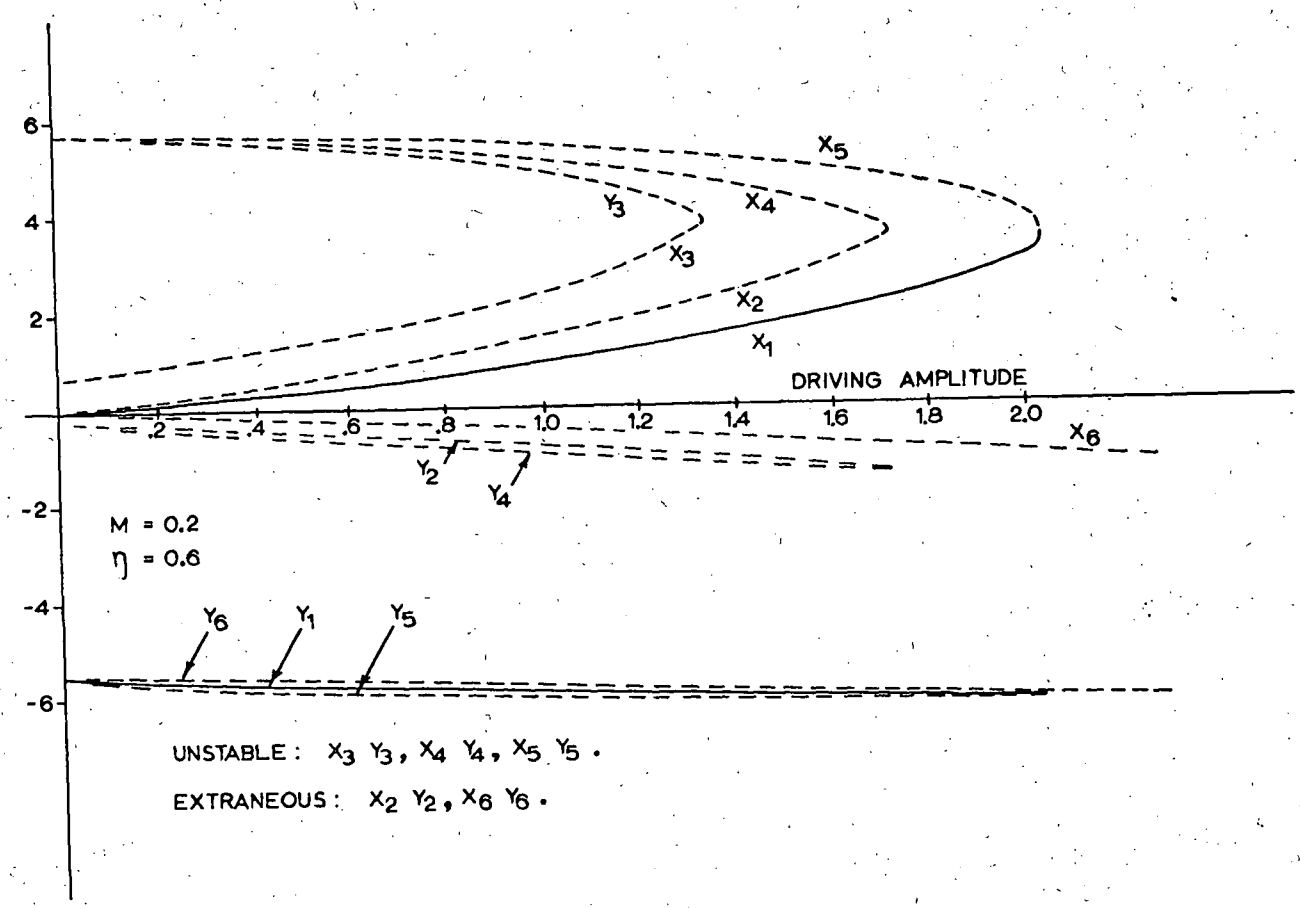

Figure 3.6 Entire Approximate Solution for Equation 3.17

insertion of the capacitor. If the circuit were now to attempt to go into the 0-0 state, less current would be drawn from the source and the voltage drop across C_s would decrease. Hence the voltage at A would increase and, as can be seen from Figure 3-5, it would tend to force the circuit back into the 0-1 or 1-0 state. Similarly, if the circuit were to attempt to go into the 1-1 state, the voltage at A would decrease and the circuit would again be forced back to the 0-1 or 1-0 state. This series capacitor can thus be used to increase the previously discussed effect of positive coupling.

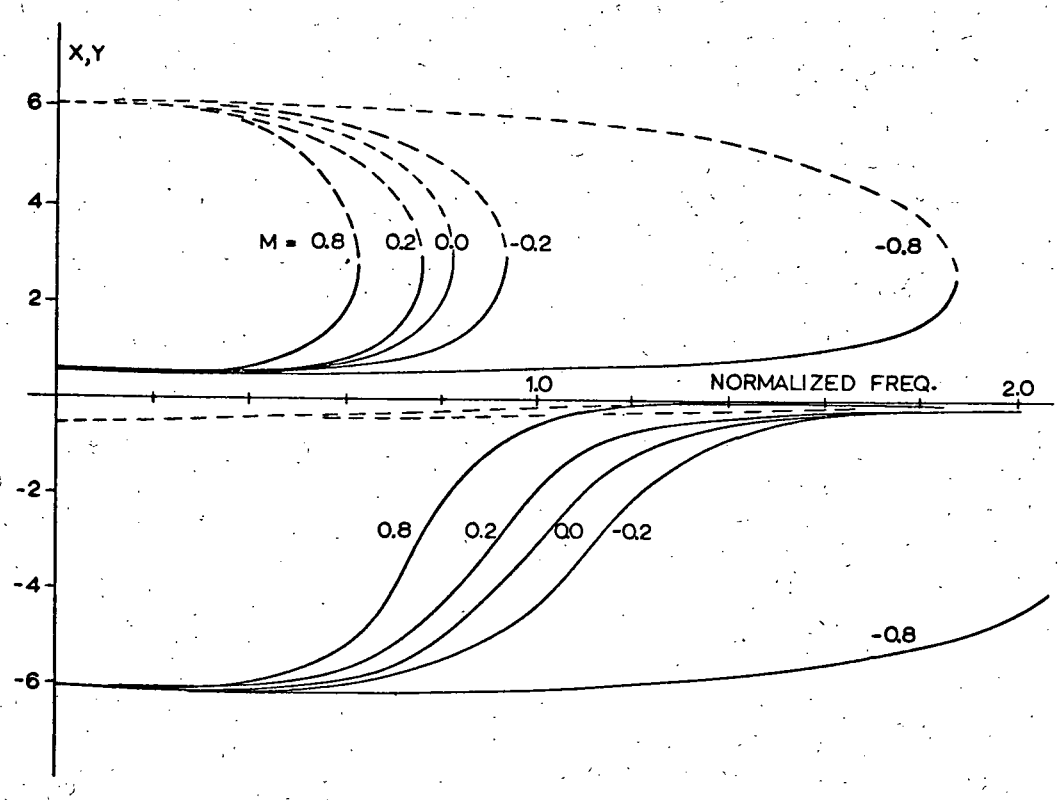

Figure 3.7 Effect of Coupling on Identical Solution Pairs

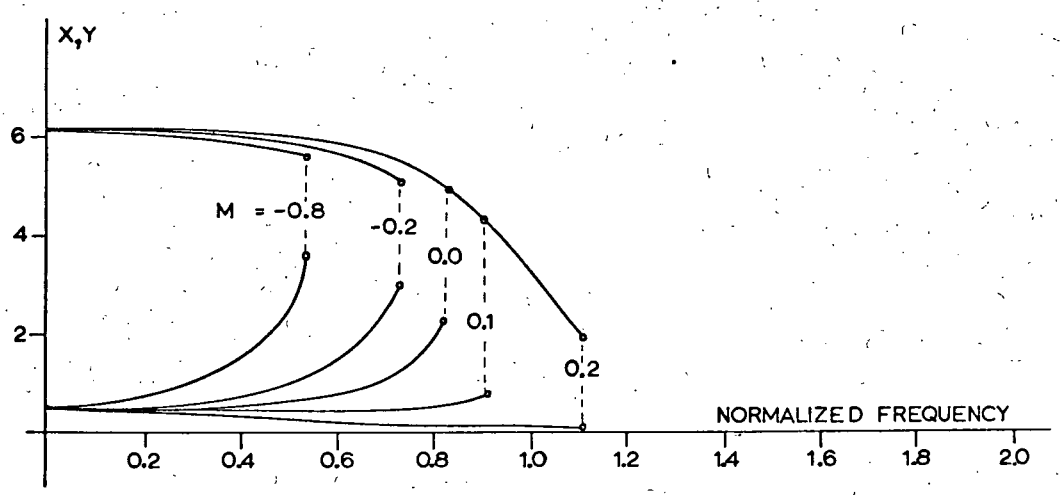

Figure 3.8 Effect of Coupling on Non-identical Solution Pairs

4. EXPERIMENTAL RESULTS

4-1 Basic Circuit Configuration

A basic circuit as shown in Figure 4-1 was constructed. The nonlinear capacitors in the resonant circuits are the Transitron SC-5 silicon capacitors that have been previously discussed and whose characteristics were used for the analogue computer study and also in the approximate analytical study of Chapter 3. As these capacitors are a type of diode, they were back-biassed at 5 volts through a 100 kilohm resistor. The carrier signal source was a General Radio Type 1001-A standard radio signal generator which was operated near the peak of the Q-curve (Figure 2-3) at 350 kHz. The inductors and transformer were wound on Siemens Siferrit ferrite pot cores which have an adjustable air gap, permitting the inductance to be varied. This feature is necessary to tune the resonant circuits to the operating frequency and also to compensate for variations in capacitance between different silicon capacitors.

4-2 Output Waveform

The output waveforms were found to be very nearly biassed sinusoids at the same frequency as the carrier source, thus validating the use of the approximate form of the solution that was used in Chapter 3. Unlike the results shown by the analogue study, higher harmonic and subharmonic responses were either non-existent or so slight that any effect they might have had on

the solutions in Chapter 3 or on the actual operation of the circuit is negligible. This apparent discrepancy between the actual circuit and its analogue model was due to the use of a slightly simplified model. It is the simplification of the frequency characteristics of the analogue model which causes the actual circuit to act more predictably than the analogue model (see Chapter 2).

4-3 Power Consumption

An approximate measurement of the steady state power consumption of the basic circuit was made by considering the whole unit as a black-box, measuring the driving voltage, and finding the current that was in phase with it in the following manner: The voltage across the unit was displayed on the vertical axis of an oscilloscope and a signal proportional to the current was displayed on the horizontal axis. From the resulting Lissajous figure the in-phase current was determined and the power dissipated by the basic circuit was calculated to be slightly less than ten microwatts. This extremely low loss is a result of this circuit consisting almost entirely of reactive components. The portion of the loss attributable to the bias resistor was less than one microwatt.

4-4 Bistability

The circuit was readily made symmetrically bistable by adding a series capacitor as discussed in section 3-8. The value of C_s was chosen such that the voltage at point A of Figure 4-1

was sufficient to permit symmetrical bistability when the signal generator was at three-quarters of its maximum output. Both sides of the circuit were tuned to the operating frequency by varying the air gap in inductors L_1 and L_2. With the circuit adjusted in this manner, the unit was symmetrically bistable with the amplitude of the high resonant state about four times that of the low one as shown by the center two traces of Figure 4-3.

4-5 Use as a Memory Device

To use a basic circuit as a memory device, all that is needed is a means of changing its state. This is readily done by applying a negative pulse through a diode at point X" or Y" in Figure 4-1. If side X is in the high resonant state and side Y is in the low state, a negative pulse at X" momentarily increases the bias on SC5-X. This increase in bias reduces its average capacitance and causes side X to drop into the low state, and because the coupling and series capacitor require that the circuit be symmetrically bistable as described, side Y is forced into the high state. Successive pulses at X" then have no further effect on the state of the circuit. To restore the circuit to its original state, a negative pulse must be applied at Y".

4-6 Use as a Counter

The circuit configuration used to demonstrate counter

operation of the device is shown in Figure 4-2. Successive pulses applied at input point A reverse the state of the circuit in a manner to be discussed in Section 4-7. The switching pulses were obtained by passing a square wave through capacitor C_2 and diode D3. Figure 4-3 shows the operation of this circuit with diode D3 shorted out. All the traces are at the same vertical scale of 1 volt/division. The upper trace shows the input triggering pulses at point A, the next two traces show the carrier envelope at points X and Y and the lower trace is of the output pulses at point Y' which are obtained by rectifying the signal at Y with diode D2 and then differentiating it with C_4, R_4. It should be noted here that with D3 shorted out, both positive and negative pulses reach point A, but only the negative pulses trigger the circuit. This effect is due to the way the circuit was tuned and will be discussed in the next section.

The sensitivity of the circuit to variations in input pulse amplitude and duration was determined by replacing the square wave generator and capacitor C_2 with a General Radio Type 1217A pulse generator. The minimum pulse duration that would reliably trigger the circuit was about 5 microseconds or nearly two complete cycles of the carrier signal. It would not be reasonable to expect the circuit to respond to a pulse duration of less than one complete cycle because the transient response would then depend on what portion of the cycle was disturbed. However, if more than one or several cycles are

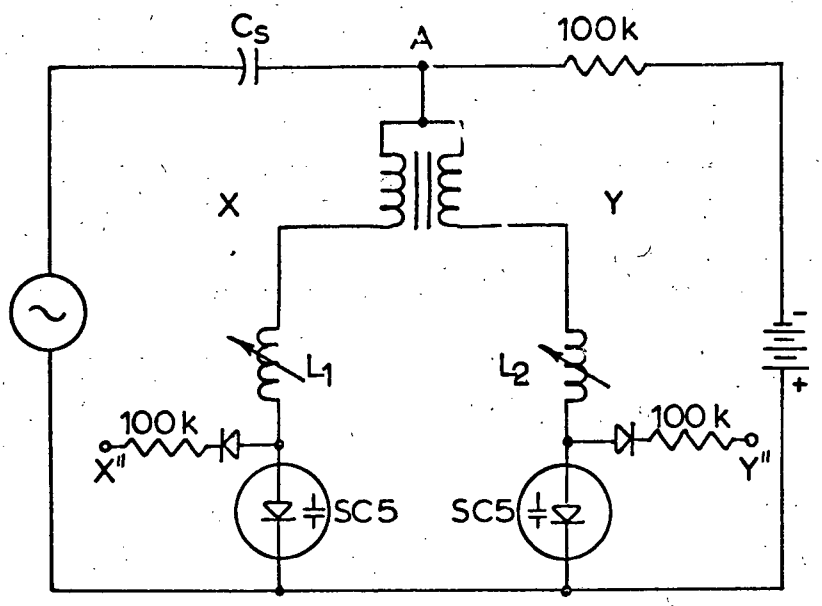

Figure 4.1 Memory Device Configuration

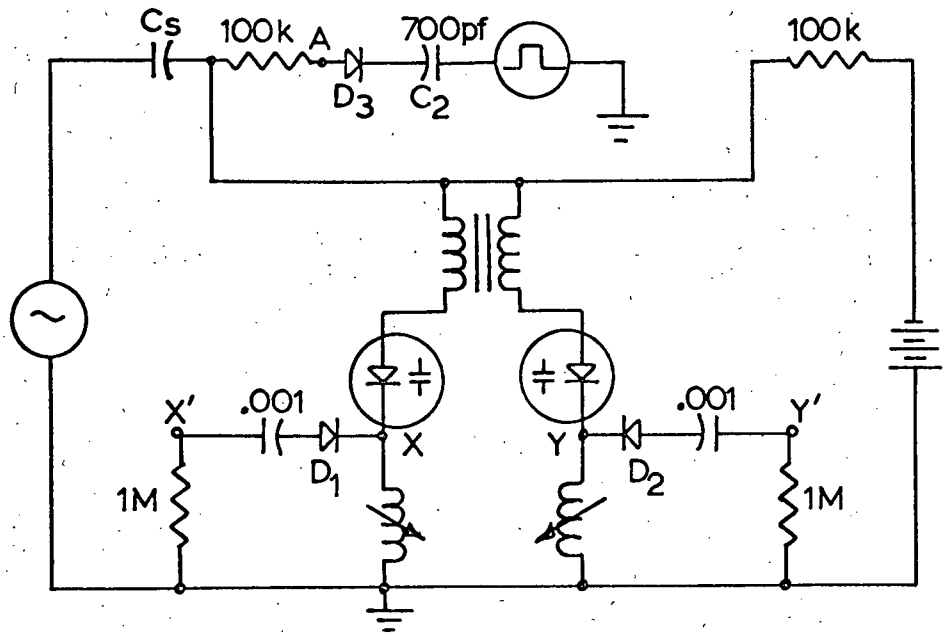

Figure 4.2 Counter Device Configuration

disturbed by a pulse, the circuit can attain a pseudo-steady state and will act as described in the next section. The minimum amplitude pulse to which the circuit would respond reliably was about 0.15 volts. This minimum amplitude of pulse is also dependent on the circuit tuning in a manner to be discussed in Section 4-7.

To trigger successive circuits, the output pulses from either X' or Y' of Figure 4-2 were used at point A of the next unit. Figure 4-4 shows the envelope at X and Y of two consecutive units. The upper two traces are of the first circuit which is triggered by negative pulses from a differentiated and rectified square wave as before, and the lower two traces are of the second unit which is triggered by output pulses as shown in the lower trace of Figure 4-3. Note the irregularities in the envelope of the second unit that occur when the first unit switches. These are a result of the 50 ohm output impedance of the signal generator which causes fluctuations in its output amplitude at switching instants. An undesirable outcome of this effect is the possible occurrence of unwanted switching which was demonstrated by placing a resistor in series with the generator to increase the output impedance as seen by the circuit. Although the impedance of the generator itself was not sufficient to adversely affect the prototype units being studied, if many such units were being driven by a single oscillator as would occur in a larger scale computing device, it would become more important that the oscillator be of low output

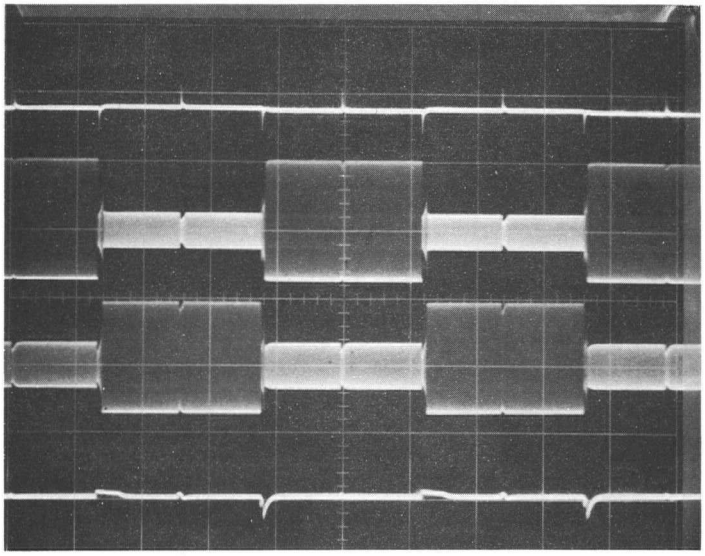

Figure 4.3 Operation of Counter

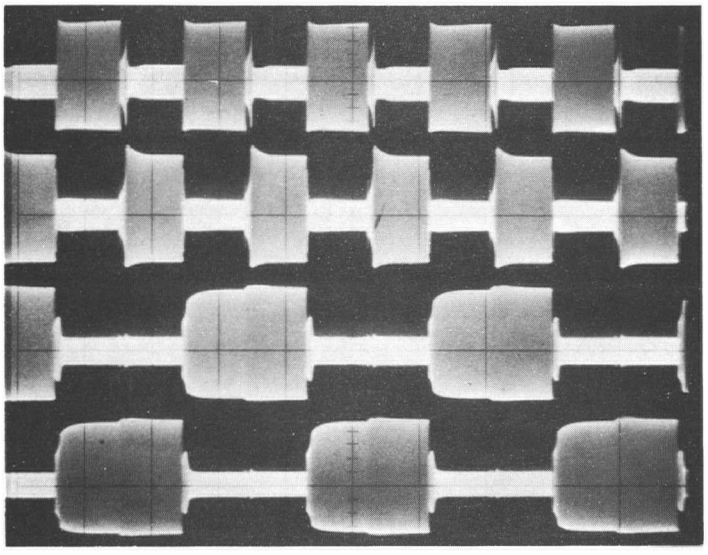

Figure 4.4 Waveforms of Two Consecutive Counters

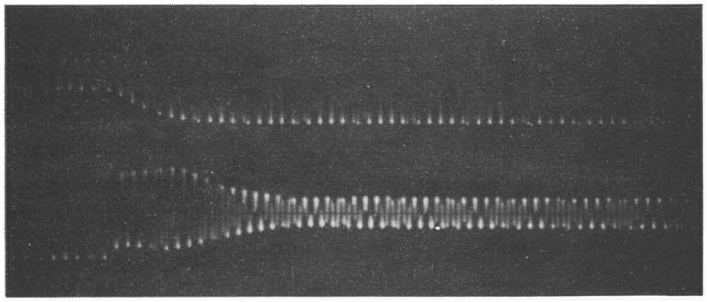

Figure 4.6 Switching Waveform

impedance.

4-7 Switching

It is not the purpose here to attempt a rigorous discussion of the transient behavicur of the circuit. Instead, an intuitive discussion based on the previously developed analytical results will be given in order to explain the process of state reversal. Suppose that initially the circuit of Figure 4-2 has side Y in the high state and side X in the low state as depicted on the solid curves of Figure 4-5a. A negative pulse applied to the nonlinear capacitors increases the bias, reducing the average capacitance, and thus shifting the frequency and amplitude response curves as shown by the broken lines in Figure 4-5a. At this instant, the only stable configuration is the 0-0 state and so Y starts to decrease. Because less current is being drawn the voltage across C_2 drops and the driving amplitude begins to increase, causing points X and Y to move as indicated. When the pulse is removed it is seen (Figure 4-5b) that Y is now in an unstable region and decreasing. Because less current is being drawn by the circuit, the voltage drop across capacitor C_s is decreased, causing the driving amplitude to be increased, and thus causing X to increase. Because the region is unstable, Y must continue to decrease until X is forced past the vertical tangency point, T_L, on the amplitude response curve (Figure 4-5b(2)), and the circuit attains the complement of its original state (Figure 4-5c). The next

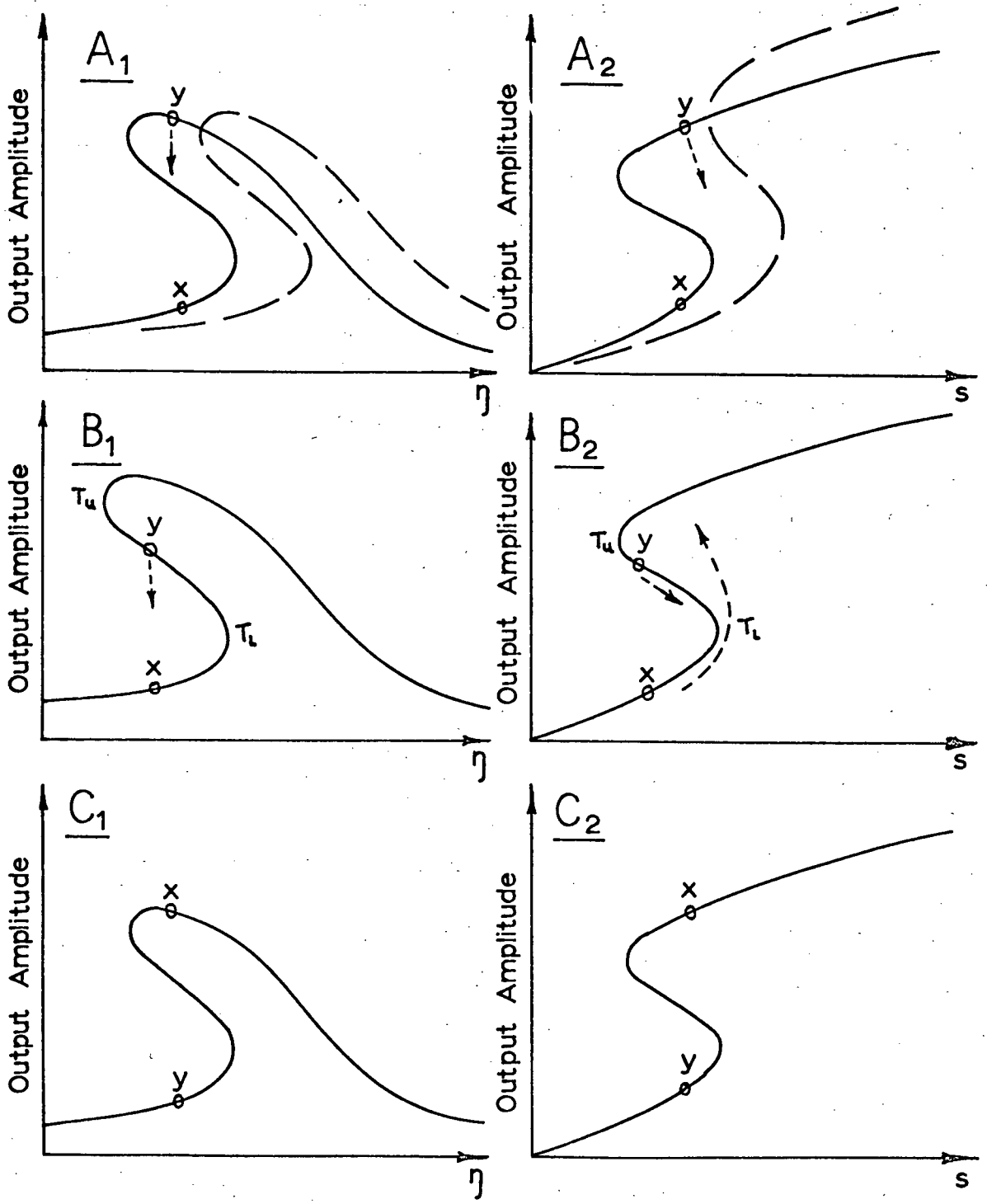

Figure 4.5 Switching Process

pulse causes a repeat of the process. From Figure 4-5a it is evident that the amplitude of the pulse required to trigger the circuit is dependent on how far the operating point is from Tu. Also, it is seen that if Y is closer to the upper vertical tangency point than X is to the lower one, as shown in Figure 4-5a, a negative pulse which shifts the frequency curve up the frequency axis will trigger the circuit more readily than will a positive pulse which shifts the frequency curve down the frequency axis. By operating the circuit at a higher frequency it is possible to use positive pulses for switching. However, the difference in amplitude between the high and low states is less in this region so it is better to use the first method with negative pulses.

The preceding discussion uses the results of the Ritz analysis which is a steady-state - not a transient-analysis. However, it can be seen from the analogue computer results (Figures 2-6, and 2-11) and also the results from the actual circuit (Figure 4-6) that the switching process takes place slowly over several cycles of the carrier signal so that at any particular instant the circuit may be considered to be in a quasi-steady state. The switching of the prototype unit (Figure 4-6) takes place over about 10 cycles of the 350 KHz carrier signal as described above and exhibits the same type of overshoot that was apparent in results obtained from the analogue computer study.

4-8 Summary

This chapter has dealt with the construction of a prototype low loss bistable circuit that has many of the properties of a conventional flip-flop. It was shown how ferroresonant circuits could be used as memory devices or cascaded to form counters. Results obtained from the actual circuit compared favorably with analogue and analytical solutions and the use of the assumed approximate solution used in the Ritz analysis was shown to be justified. Finally, a description of the switching process was given which combined a consideration of the Ritz results with observable features of the analogue and circuit switching waveforms.

5. CONCLUSIONS

The purpose of this work was to study jump resonance phenomena and to investigate the possibility of using the principle in the design of digital logic elements. The system chosen for study was described by a pair of nonlinear second order differential equations which were coupled by second derivative terms and were driven by a sinusoidal forcing function. Klotter's work on the Ritz method of analysis was extended to study the previously mentioned coupled equations with asymmetrical nonlinearities. Klotter's work was limited to symmetrical nonlinearities in equations with coupling and the coupling was only in the dependent variable. The analysis yielded algebraic conditions which were solved on a digital computer to obtain frequency and amplitude responses of the model.

The results of the above study compared favorably with those obtained from the study of a model on an analogue computer, and information from the two studies was used in the design and construction of a prototype bistable circuit which used low and high resonant states of jump resonant circuits to represent a 0 and 1 basis for logical operations. The prototype circuits had many of the features of conventional flip-flops such as being able to store and count binary numbers and drive other units. However, unlike conventional flip-flops, they required an ac driving source as well as a dc bias supply.

The dc bias supply could be eliminated from the circuit with the advent of nonlinear capacitors with a dielectric such as barium titanate. Such capacitors would be of low loss, and have a nonlinear characteristic. These ferroelectric devices have been successful in parametric amplifiers.

Another problem inherent in the device studied was the switching time. It was very dependent on the carrier frequency and also on the loss of the circuit. It was shown by the analogue computer study that switching would not occur reliably in less than five cycles of the carrier signal and that ten cycles would be more useful as a design minimum. The implication here is that the driving source must consist of an oscillation at a frequency at least ten times the desired maximum switching rate. The cutoff frequency of the nonlinear capacitor sets the maximum operating frequency of the resonant circuit and therefore the maximum switching speed. For low speed applications conventional lumped elements can be connected together to form logic circuits such as was done with the prototypes described in this report, but for higher operating frequencies it would become increasingly difficult to contain the signals in or near the elements and lines. One way of avoiding this problem would be to use conventional microwave devices such as coaxial cables, waveguides and resonant cavities. However, these are quite large and cumbersome. Another possible way of increasing the switching speed would be to make the size of the device small

compared to one wavelength. The technique of microminiaturization is still under development and it would be useful for future workers in that field to consider miniaturizing the circuits developed here.

The main incentive for future work along these lines is the inherent low power consumption of the devices. Because most of the components needed are of a reactive nature, loss is primarily due to capacitor leakage and copper and core loss in the inductive elements. Devices of the type developed here would find application in situations where logical operations are required and where low power consumption is necessary.

In summary, the work presented here includes:

1. Extending previous work on the Ritz method of analysis so as to permit study of coupled nonlinear differential equations which have asymmetrical nonlinearity.
2. An analogue computer study of a model of a bistable ferroresonant circuit.
3. The design and construction of a prototype of the above circuit, and some suggestions for future study.

APPENDIX A

Polynomial Approximation to the f(q) Characteristic for the Silicon Capacitor

The voltage-capacitance characteristic of the Transitron SC-5 silicon capacitors (Figure 2-2) was tabulated and using this data a polynomial approximation to the f(q) in (3-4) was made using a least squares fitting procedure. A brief outline of that procedure follows.

The charge on the capacitor can be described by

$$q = v \cdot C(v) \qquad \text{(A-1)}$$

The voltage v, and the corresponding capacitance, C(v), were found at 52 points in the voltage range 0 to -30 volts. Quadratic and cubic least squares fits were made at -5 volt bias to

$$v = f(q) = a_o + a_1 q + a_2 q^2 + \ldots . \qquad \text{(A-2)}$$

The results are tabulated in Figures A-1, A-2, and Table A-1. Both the quadratic and the cubic approximations to the characteristic are well within the 20% variation among components that is claimed by the manufacturer. As a result, the quadratic approximation is used in the analysis in Chapter III.

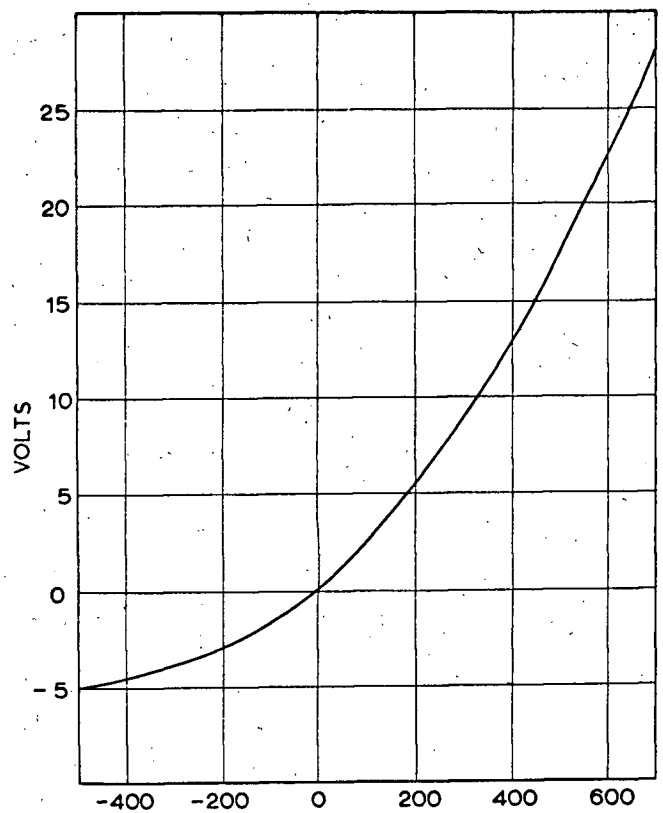

Figure A.1 Normalized f(q) Characteristic

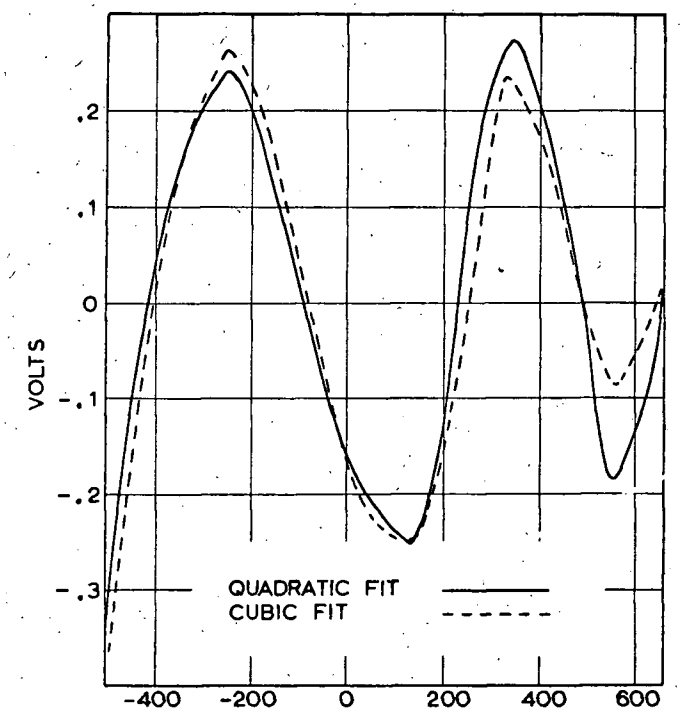

Figure A.2 Deviation Between f(q) and the Polynomial Approximations

Coefficient Approximation	a_o	a_1	a_2	a_3	Standard Deviation
Quadratic	1.65×10^{-1}	2.30×10^{-2}	2.68×10^{-5}	--	0.1737
Cubic	1.43×10^{-1}	2.32×10^{-2}	2.70×10^{-5}	-8.6×10^{-10}	0.1722

Table A.1

APPENDIX B

Determination of the Ritz Coefficients

Figure B-1 is the flow diagram depicting the procedures followed in determining the dependence of the Ritz coefficients on the various parameters of interest. The program is quite versatile and portions of it are self-checking. Laguerre's method of finding polynomial roots[15] gives quick convergence from any starting value for distinct roots. One Laguerre step requires more calculation than one Muller, Newton, or Bairstow step, but with no a priori approximation to the zeroes it more than compensates for this by the reduction in the number of iterations needed. If the root is simple, convergence is cubic; otherwise it is linear. The actual Fortran program used is a modified form of the program "LAGERE" which was written by J. Stevens[16] in 1966 and has since been added to the computing center's library. The modifications made to this program allow it to be used to find small roots with a high degree of accuracy and also to check its accuracy by reconstructing the coefficients from the roots. These modifications were necessitated by the properties of polynomials (3-13) and (3-17) and by the requirement that the root-finding technique be operative over a wide range of coefficient values.

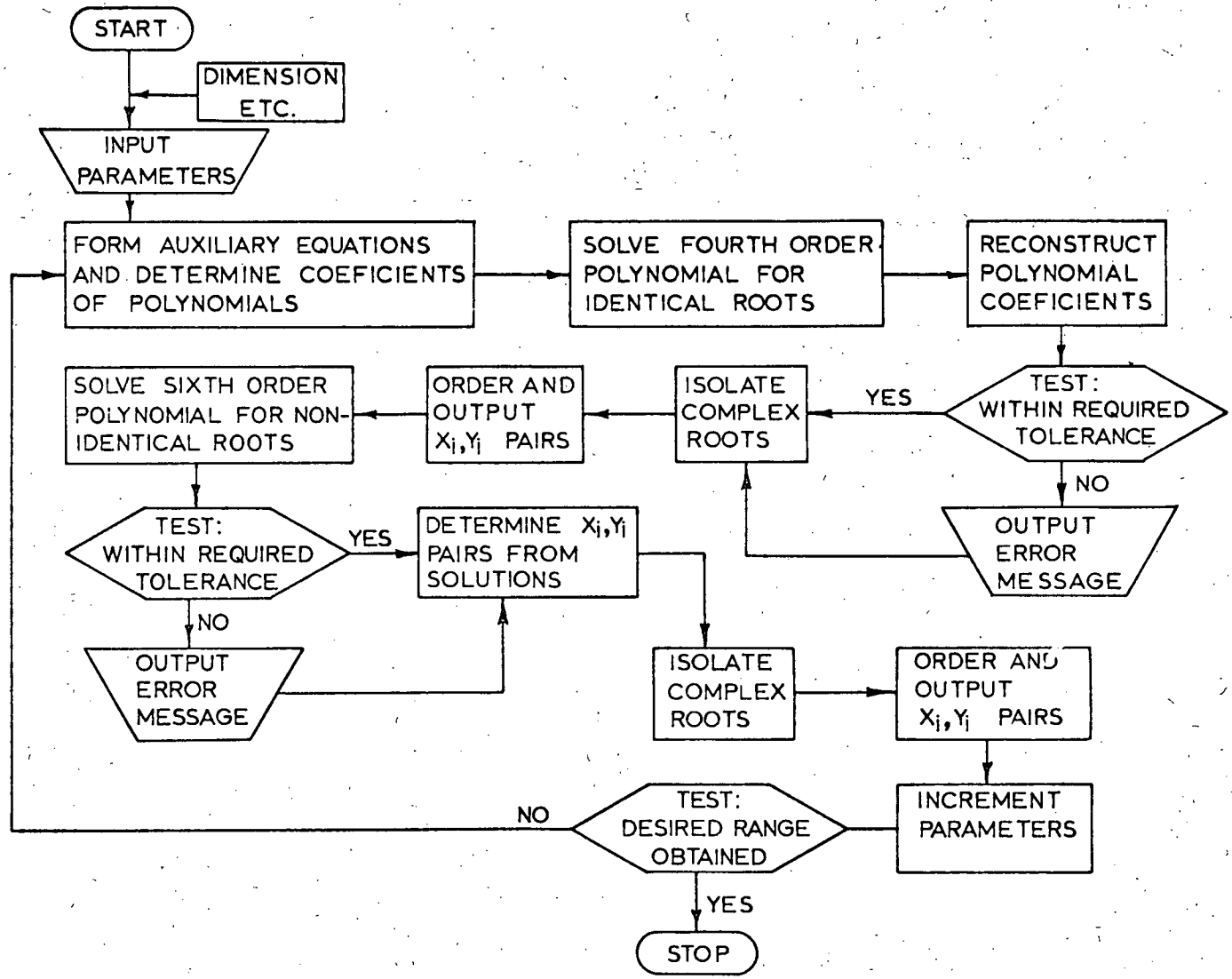

Figure B.1 Flow Diagram of Program to Determine Ritz Coefficients

REFERENCES

1. Rouelle, E., "Contribution à l'étude expérimentale de la ferro-résonance", Revue Generale de l'Electricité, 36: pp. 715-738, 763-780, 795-819, 841-858, 1934.

2. Rüdenberg, R., Transient Performance of Electric Power Systems, McGraw-Hill, 1950.

3. Lenkurt Electric Co., Selected Articles from The Lenkurt Demodulator (Second Edition), "The Varactor Diode", pp. 667-677, 1966.

4. Stoker, J., Nonlinear Vibrations, N.Y., 1950.

5. Hayashi, C., Nonlinear Oscillations in Physical Systems, McGraw-Hill, 1964.

6. Isborn, C., "Ferroresonant Flip-flops", Electronics, April 1962, pp. 121-123.

7. Gremer, C., "The Nonlinear Resonant Trigger Pair", Tran. AIEE. Communications and Electronics, Vol. 26, Sept. 1956, pp. 404-407.

8. Ozawa, T., Nonlinear Resonance Computer Components, Tech. Report No. 1306-1, Stanford Electronics Laboratories, April 1963.

9. Klotter, K., "Steady State Vibrations in Systems Having Arbitrary Restoring and Arbitrary Damping Forces", Proc. of the Symp. on Nonlinear Circuit Analysis, Vol. 2, Polytechnic Institute of Brooklyn, N.Y., pp. 234-257, 1953.

10. Klotter, K., "Steady State Oscillations in Nonlinear Multi-Loop Circuits", Trans. Inst. of Radio Engineers, Prof. Group on Circuit Theory, CT-1, No. 4, pp. 13-18, Dec. 1954.

11. Zeniti, K., Sekiguti, S., and Takasima, M., "Parametric Excitation using Variable Capacitance of Ferroelectric Materials", Journal of the Inst. of Elect. and Communication Engineers of Japan, Vol. 41, No. 3, March 1958, pp. 239-244.

12. Jackson, A., Analog Computation, McGraw-Hill, pp. 182-185, 1960.

13. Cunningham, W., Introduction to Nonlinear Analysis, McGraw-Hill, 1958.

14. Ritz, W., Über eine neue Methode zur Lösing gewisser Variationsprobleme der mathematischen Physik", Crelles Jour. f.d. reine u. ang. Math., Vol. 135, pp. 1-61, 1909.

15. Parlett, B., "Laguerre's Method Applied to the Matrix Eigenvalue Problem", Mathematics of Computation, Vol. 18, 1964, pp. 464 ff.

16. Stevens, J., "LAGERE", Unpublished Fortran program, U.B.C. Computing Center Library, 1966.